SUPPLEMENTAL INFORMATION

Bulk Recrystallization for Efficient Mixed-Cation Mixed-Halide Perovskite Solar Cells

Liangyou Lin†[a,b], Jacob Tse-Wei Wang†[a], Timothy W. Jones[a], Mihaela Grigore[c], Andre.Cook[a], Dane W. deQuilettes[d], Roberto Brenes[d], Benjamin C. Duck[a], Kenrick F. Anderson[a], Noel W. Duffy[e], Bernard Wenger[f], Vladimir Bulović[d], Jian Pu[b], Jian Li[b] , Bo Chi[b], Henry J. Snaith[f], Gregory J. Wilson*[a]*

†These authors contributed equally to this work.

[a]CSIRO Energy, Newcastle Energy Centre, 10 Murray Dwyer Cct, Mayfield West, NSW 2304, Australia.
[b]Center for Fuel Cell Innovation, School of Materials Science and Engineering, Huazhong University of Science &Technology, Wuhan 430074, China
[c]CSIRO Energy, 11 Julius Avenue, North Ryde 2113, Australia
[d]Research Laboratory of Electronics, Massachusetts Institute of Technology, 77 Massachusetts Avenue, Cambridge, Massachusetts 02139, USA
[e]CSIRO Energy Clayton Laboratories, Clayton, Vic 3168, Australia.
[f]Clarendon Laboratory, University of Oxford, Parks Road, Oxford, OX1 3PU, UK
**Corresponding author: Greg.Wilson@csiro.au (G.J.W.); chibo@hust.edu.cn (B.C.)*

EXPERIMENTAL METHODS

Materials

All chemicals were purchased from Sigma Aldrich, Tokyo Chemical Industry (TCI) or Greatcell Solar and used as received unless stated otherwise.

Devices preparation

Devices were fabricated on fluorine-doped tin oxide (FTO) coated glass substrates (Pilkington). Substrates were cleaned sequentially with 2% Hellmanex, deionized water and isopropanol in an ultrasonic bath for 30 min, after rinsing with isopropanol the substrates were further cleaned with air plasma for 30 min.

Electron transport layer preparation

SnO_2 layer was prepared following the method described in the literature.[1] A 17.5mg mL^{-1} precursor solution was prepared by dissolution of after 30 min stirring at room temperature, it was deposited on cleaned FTO substrates with 2000 rpm spin rate for 30 s with a 1000 rpm s^{-1} acceleration, followed by pre-drying at 100 °C for 10 min and then heat-treated at 180 °C for one hour. SnO_2 layer was post-treated by the chemical bath, where 2.5 g urea was dissolved in 200 ml deionized water (which was pre-heated to 70 °C), followed by addition of 50 µL 3-mercaptopropionic acid, 2.5 ml HCl (37 wt %) and 540 mg $SnCl_2{\cdot}2H_2O$. The deposition was made by putting the substrates in a glass container pre-heated to 70 °C filled with the pre-made solution, then kept in a 70 °C oven for 2 h. The treated substrates were rinsed with deionized water, dried by nitrogen-gun and annealed for another 1 h at 180 °C. All SnO_2 layers were treated with air plasma for 20 min before deposition of the perovskite films. The PCBM (Solenne, 5mg mL^{-1} in chlorobenzene) solution was spin coated at 5000 rpm for 30 s with 5000 rpm s^{-1} acceleration on top of the SnO_2. The substrates were then annealed at 100 °C for 10 mins in a nitrogen-filled glove box. Note: devices shown in Fig. 4 and Fig. S11

were made with a slightly modified method, starting with 0.1M $SnCl_2 \cdot 2H_2O$ precursor spincoating deposition on FTO/Glass substrates at 4000 rpm for 30 s , followed by annealing at 180°C for 60 min. Then a layer of SnO_2 colloid precursor (diluted by H_2O, v:v=1:6) was spin coated onto SnO_2/FTO-glass substrates at 4000 rpm for 30 s, and annealed at 150 °C for 30 min.

Perovskite precursor solution and films preparation

The perovskite films were deposited from a precursor solution containing cesium iodide CsI (0.065M) formamidinium iodide FAI (Dyesol, 1.050 M), lead iodide PbI_2 (TCI, 1.205 M), methylammonium bromide MABr (Dyesol, 0.185 M) and lead bromide $PbBr_2$ (0.195 M) in a mixture of anhydrou dimethylformamide:dimethylsulfoxide (DMF:DMSO) 4:1 (v: v). The perovskite solution was spincoated using a two-step program at 2000 rpm and 4000 rpm for 10 s and 20 s with 200 $rpms^{-1}$ and 1000 rpm s^{-1} acceleration, respectively. During the second step, 300 µL of chlorobenzene was fully pipetted to the spinning substrate 1 s prior to the end of the program. The substrates were then annealed at 100 °C for 30 min in a nitrogen-filled glove box. For FACl treatment, after 30 min cooling of substrate to room temperature, the FACl/isopropanol solution was dropped onto the primary perovskite surface via dynamic spin-coating, followed by annealing the film at 100 °C for a further 5 min.

Hole transport layer and top electrode deposition

After the perovskite film was annealed, the substrates were cooled down for at least 10 minutes and a spiro-OMeTAD (Dyesol) solution was spin-coated at 4000 rpm for 20 s with 4000 rpm s^{-1} acceleration. The spiro-OMeTAD solution was prepared by dissolving 72.3 mg spiro-OMeTAD, 17.5 µl 520 mg mL^{-1} bis (trifluoromethane) sulfonimide lithium salt (Li-TFSI) in acetonitrile and 28.8 µl 4-tert-butylpyridine (tBP) in 1 ml anhydrous chlorobenzene.

Afterwards, the film was stored overnight (more than 16 hrs) in a desiccator; finally 60 nm Au was thermally evaporated to form the top contact of the solar cells.

Device Characterization

The current–voltage (*I*–*V*) characteristics of the cells were recorded with a digital source meter (Keithley model 2400, USA) in a 4-terminal connection. A 450 W Newport Oriel class AAB xenon lamp was used as the light source for photovoltaic (*j*–*V*) measurements. The solar simulator intensity was confirmed against a calibrated Si reference cell (Fraunhofer), checked and recorded before each measurement. Typically, the devices were fabricated with a evaporated contact area of 0.10 cm^2 and measured with 0.08 cm^2 size aperture unless stated otherwise. Scan sweep rate was performed at 100 mV s^{-1} and no device preconditioning such as light soaking, or forward voltage bias, was applied before starting the measurement. Electrochemical impedance spectroscopy (EIS) were measured with an Autolab PGSTAT 302N potentiostat/galvanostat fitted with an impedance spectroscopy module. Illumination was provided by a white light LED. Film thickness was measured with a Dektak 1500 profilometer (Veeco Instruments).

Thin-Film Characterization

Scanning Electron Microscopy (SEM) analyses were performed using a field emission SEM (Zeiss Auriga FIB-FESEM), operated at an accelerating voltage of 5 kV with In-Lens secondary electron detector. Phase analysis of the films was performed on a PANalytical Empyrean X-ray diffractometer using CuKα radiation at 40 kV and 40 mA. The analyses were carried out using two configurations of the X-ray diffraction (XRD) such as Bragg–Brentano geometry (symmetric scan) and grazing incidence XRD (GIXRD) (asymmetric scans). To prevent the degradation of the samples during the analysis, an XRK-900 reactor chamber (Anton Paar) was used to keep the samples under N_2 flow. Step scans were undertaken from 8 to 70° 2θ,

with a step interval of 0.007° 2θ. The asymmetric scans were run at different incident beam angles ranging from 0.2° to 1.2° 2θ and an increment of 0.1°.Perovskite samples were prepared on glass and coated with an inert polymer poly(methyl-methacrylate), PMMA. Time-resolved photoluminescence decays were acquired following previous reports using a time-correlated single photon-counting set-up (FluoTime 300, PicoQuant).[2] Samples were photoexcited using a 507-nm laser head (LDH-P-C-510, PicoQuant) with pulse duration of 117 ps, fluence of ~30 nJ/cm^2 per pulse and a repetition rate of 0.2-1 MHz. Photoluminescence Quantum Efficiency (PLQE), steady-state photoluminescence quantum efficiency values were determined using a 532 nm constant wave (CW) laser excitation source (Suwtech LDC-800) to illuminate a sample in an integrating sphere (Oriel Instruments 70682NS), and the laser scatter and PL were collected using a fiber-coupled detector (Ocean Optics MayaPro). The spectral response of the fiber-coupled detector setup was calibrated using a spectral irradiance standard (Oriel Instruments 63358). PLQE calculations were carried out using an established technique reported previously.[3] Optical microscopy was performed using a sample-scanning confocal microscope built around a Nikon Eclipse-Ti inverted microscope fitted with an infinity corrected 100× dry objective (Nikon Plan Epi, NA = 0.85). The excitation wavelength was set at 532 nm by wavelength selecting the broadband emission from a supercontinuum laser (NKT Photonics SuperK Extreme, 40 MHz, 100 nJ cm^{-2} per pulse) sent through an acousto-optic modulator (NKT Photonics Supertrek dual, ~3 nm bandwidth) driven by a radio-frequency function generator (Stanford Research Instruments, Inc. Model SG382) and amplifier at a frequency of 116 MHz. The sample emission was filtered through a 532 nm laser BrightLine single-edge laser-flat dichroic beamsplitter (Semrock DiO2-R532) and directed to a Micro Photon Devices PDM series single-photon avalanche photodiode with a 50 µm active area. The sample stage (Physik Instrumente, P-733.3CL) was controlled using a

piezo controller (Physik Instrumente, E-710.4CL) with a pixel size of 39 nm and dwell time (integration time) of 10 ms. Time-correlated single photon counting was performed with a PicoHarp 300 and fluorescence lifetime images were collected using the SymPhoTime 64 software package (Picoquant GmbH). Before measurements, the system was calibrated using 200 nm fluorescent microspheres (Lifetechnologies FluoSpheres Polystyrene Microspheres, 200 nm diameter, Suncoast Yellow, 540/600 nm)

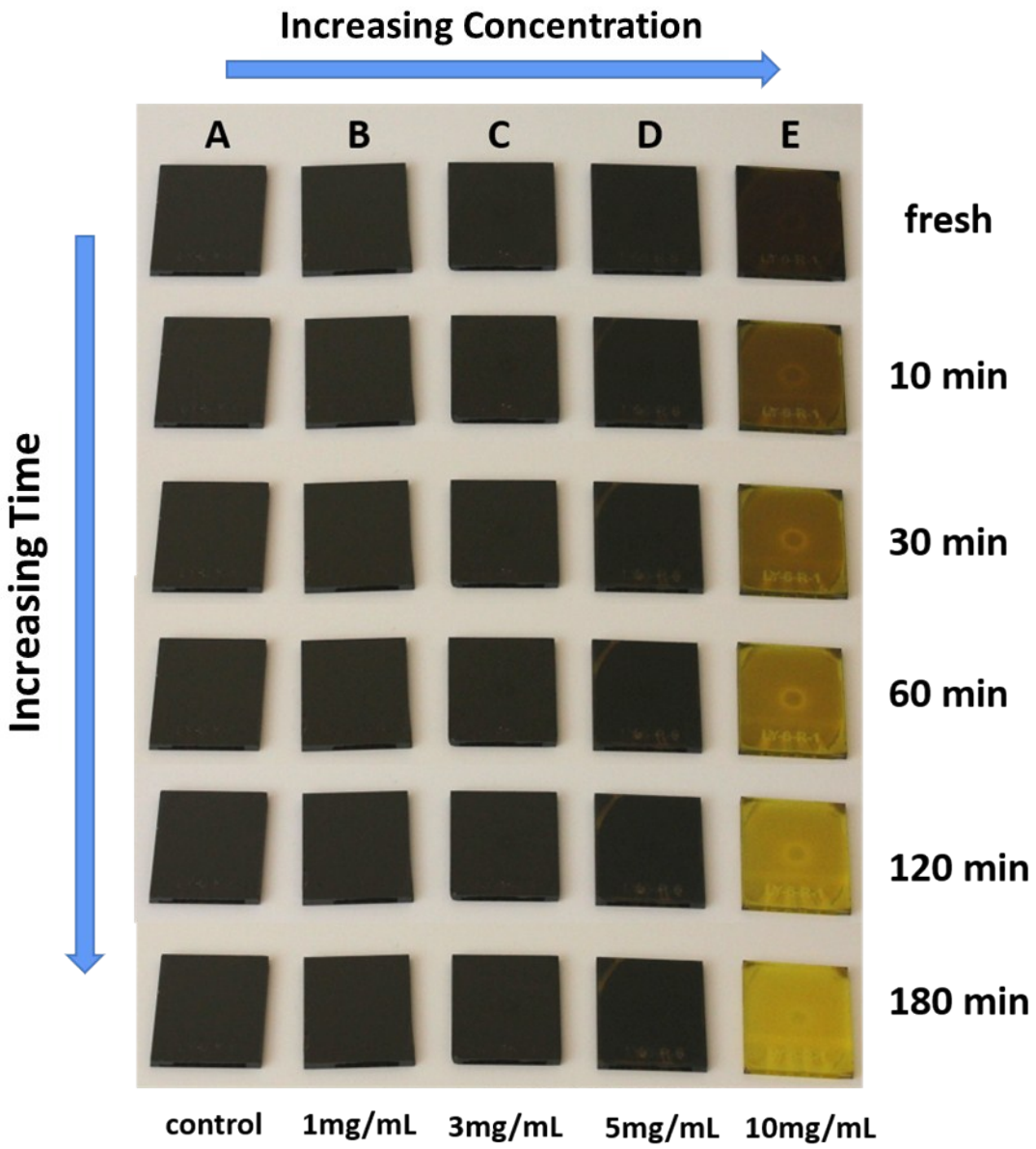

Fig. S1. Images of the Control and a series of FACl-treated perovskite films (up to 10 mg/ml) exposed in air (RH~65%, T~25 °C) with different time.

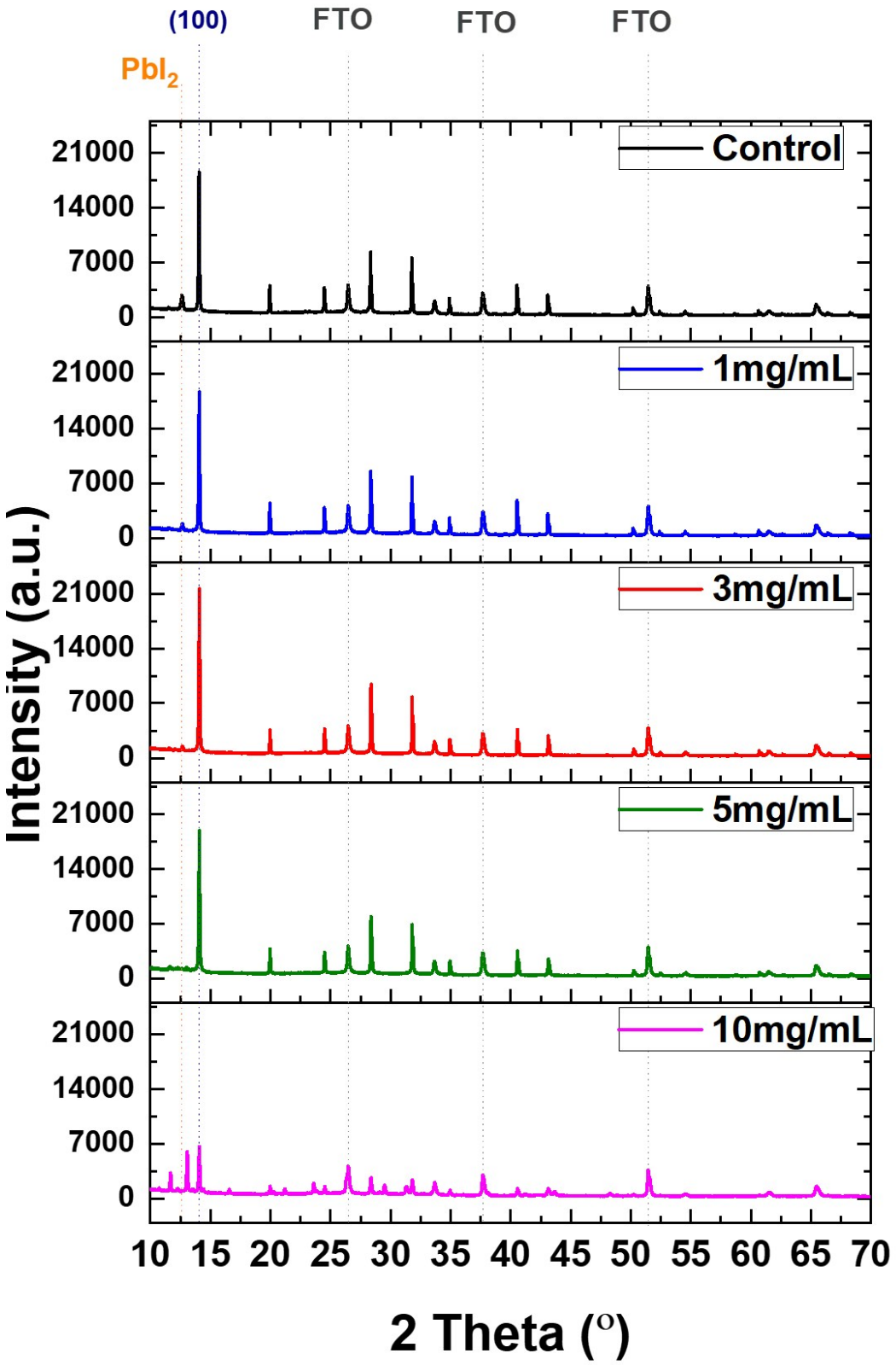

Fig. S2. X-ray diffraction patterns acquired using Bragg–Brentano geometry of a series of FACl loading on perovskite thin films.

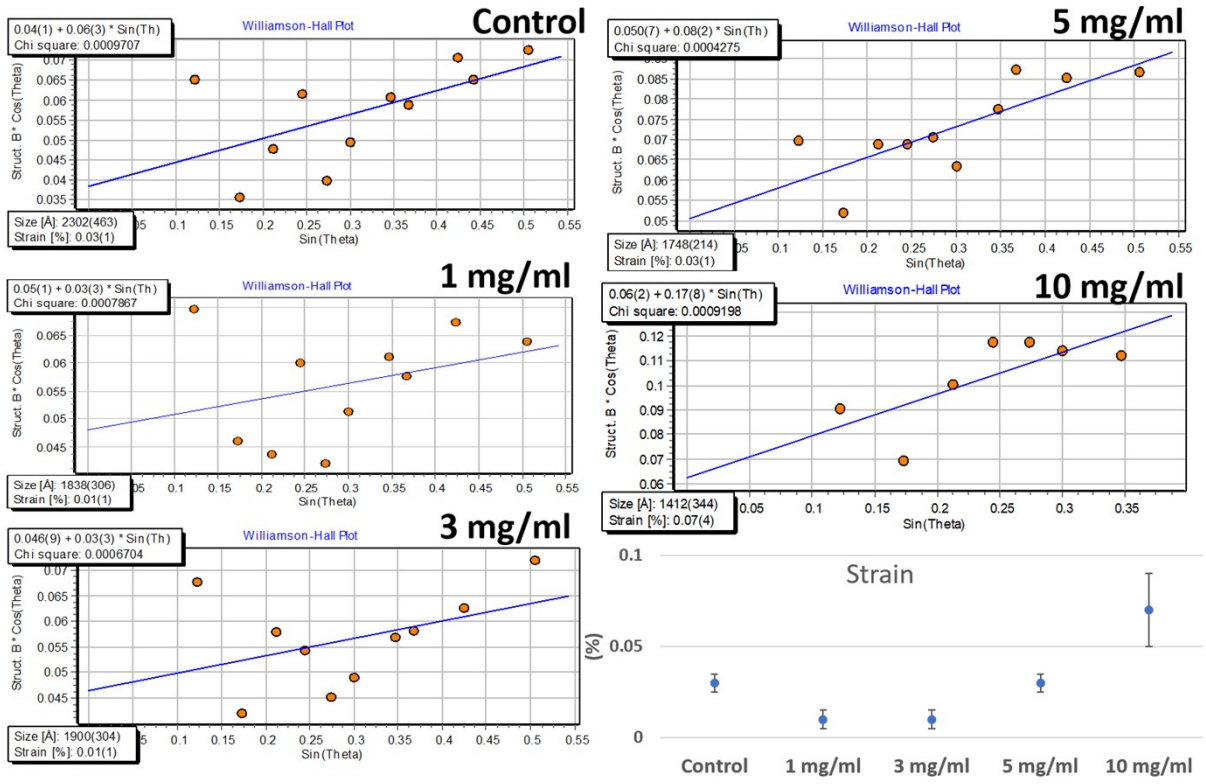

Fig. S3. Williamson-Hall plots for the control and a series of FACl loading on perovskite thin films. The equation of the line and the quality of the fit are shown in the upper-left corner of the plot. The average strain and size of the perovskite crystals are shown in the lower-left corner of the plot. The standard deviation for both strain and size is shown in the brackets for the last digits.

Calculation of Williamson-Hall relationships in Fig. S3

$$B = \frac{K\,\lambda}{L\cos\theta} + 4\,\varepsilon\frac{\sin\theta}{\cos\theta}$$

$$B\cos\theta = \frac{K\,\lambda}{L} + 4\,\varepsilon\sin\theta$$

L – crystallite size
K – Scherrer constant
B – Full Width at Half Maximum (FWHM)
λ – wavelength
ε – strain

The microstrain of the perovskite crystals in films was determined using Line Profile Analysis (LPA). HighScore Plus, a Panalytical software, was used to perform a profile fit to the measured XRD patterns. The XRD patterns used for the LPA analysis had the Signal-to-Noise ratio (SNR) for the maximum intensity peak ranging between 93 and 316 (Table S1). The instrumental broadening present in the measured patterns was removed using the XRD

pattern of a standard sample (LaB_6). The goodness of fit (Chi^2 value) of the calculated profiles over the measured patterns are given in Table X. A Chi^2 value less than 4 indicates a well refined pattern.

Sample	SNR	Chi^2
Control	268	1.42
1 mg/ml	254	1.38
3 mg/ml	316	1.25
5 mg/ml	261	1.28
10 mg/ml	93	1.08

Table S1. – The Signal-to-Noise ratio (SNR) for the maximum intensity peak of the measured XRD patterns and the goodness of fit of the calculated profiles with different perovskite samples (different FACl loadings)

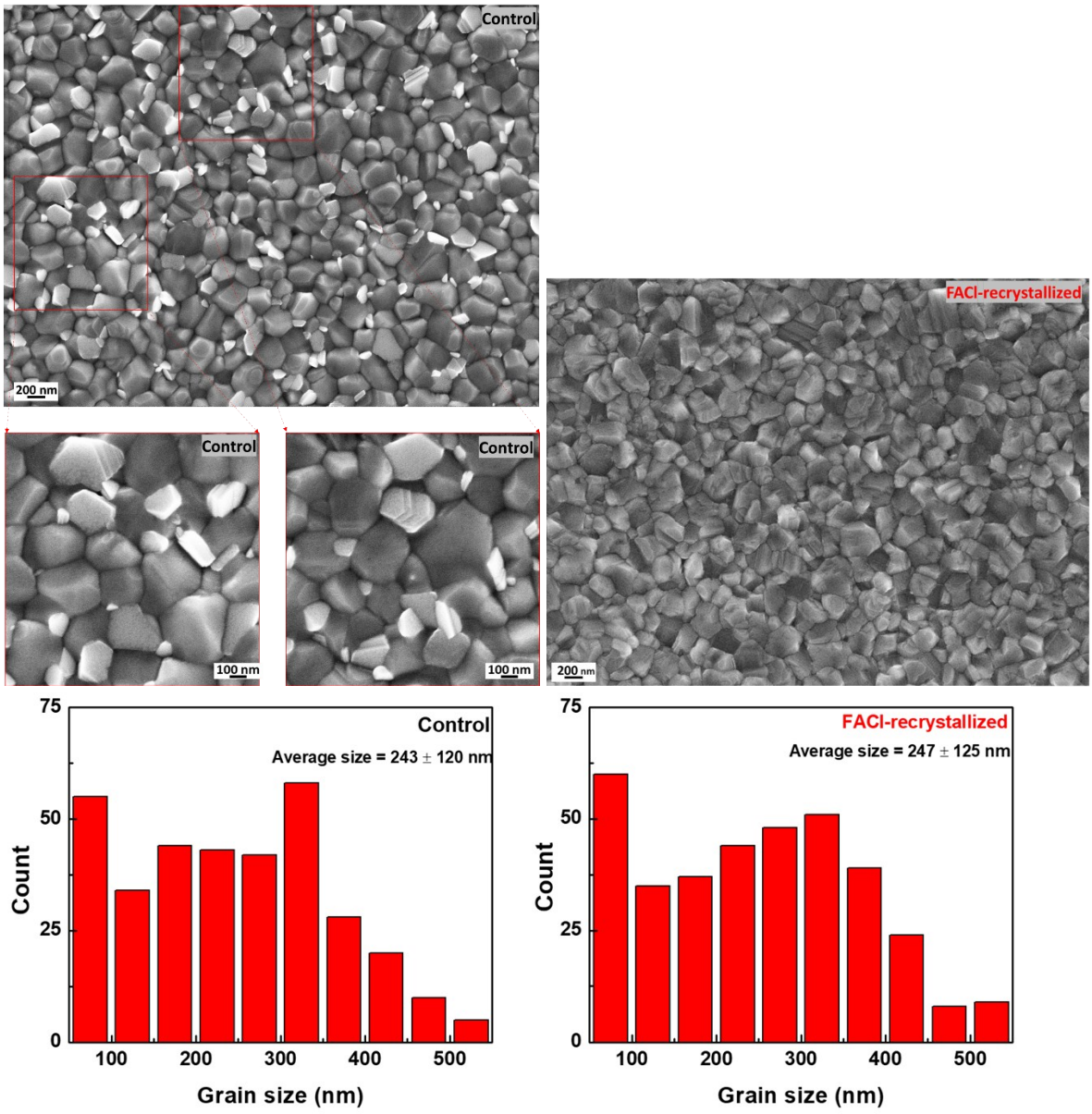

Fig. S4. Scanning electron micrographs of perovskite samples and their grain size distrubution statistics analyzed from corresponding images..

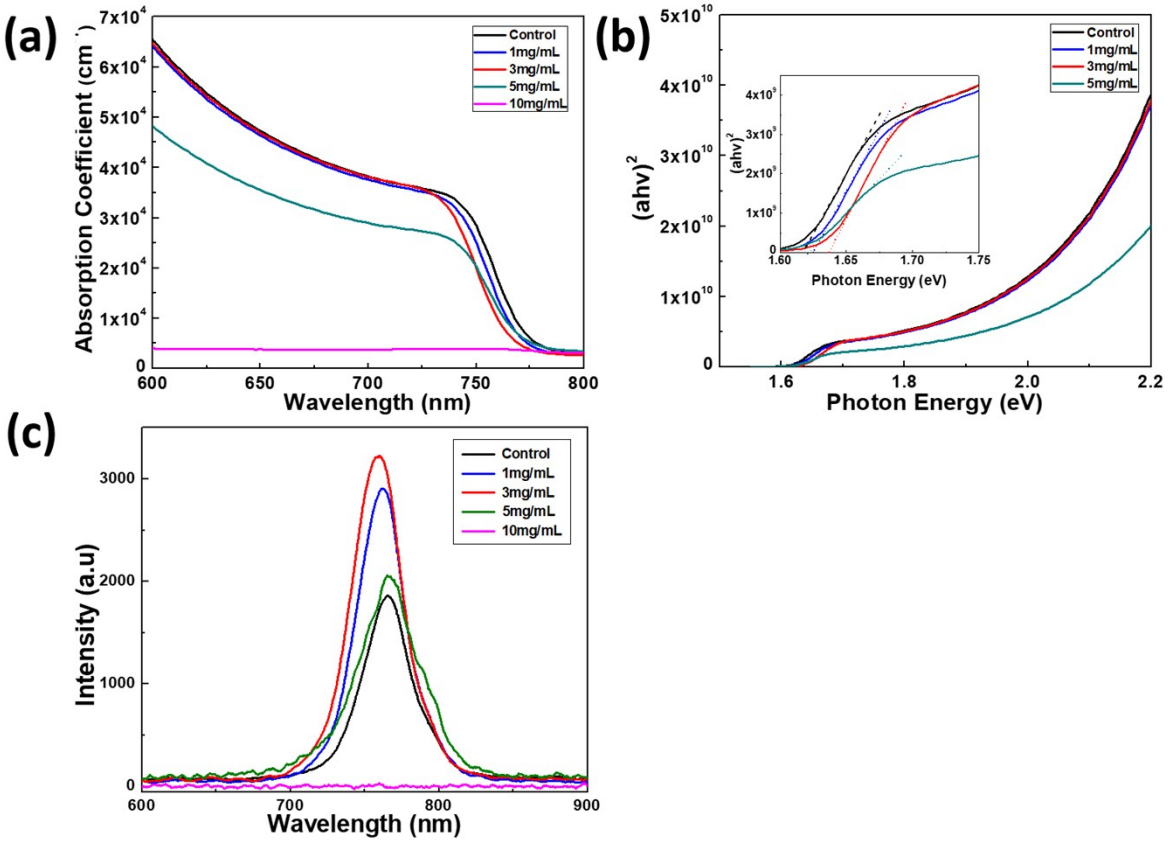

Fig. S5. (a) UV-vis absorption coefficient (α) of perovskite films. (b) Band-gap estimation from absorption coefficient. (c) Steady-state photoluminescence spectra of perovskite films. The Urbach energy and band-gap with 10 mg mL^{-1} FACl loading are not available here due to the rapid degradation happened throughout the experiments.

Calculation of Absorption coefficients for data in Fig. S5

The absorption coefficient (α) is calculated by applying the empirical formula as:

$$\alpha = \frac{-1}{t}\ln\left(\frac{T}{1-R}\right) \qquad (1)$$

where *t* is the thickness of the film, *R* is the reflectance, and *T* is the transmittance. The thickness of films are measured by depth profiler as 534 ± 8 nm and 555 ± 5 nm for control and FACl-treated sample, respectively. The two perovskite films have been found to have comparative absorption coefficient. Their band-gap (E_g) has been determined by using Tauc's relationship:

$$(\alpha h\nu)^2 = \alpha_0 (h\nu - E_g) \qquad (2)$$

in the high absorption region of direct band gaps semiconductor, where α_0 is an energy independent constant, sometimes referred as the band tailing parameter, *h*υ is the incident photon energy.[4]

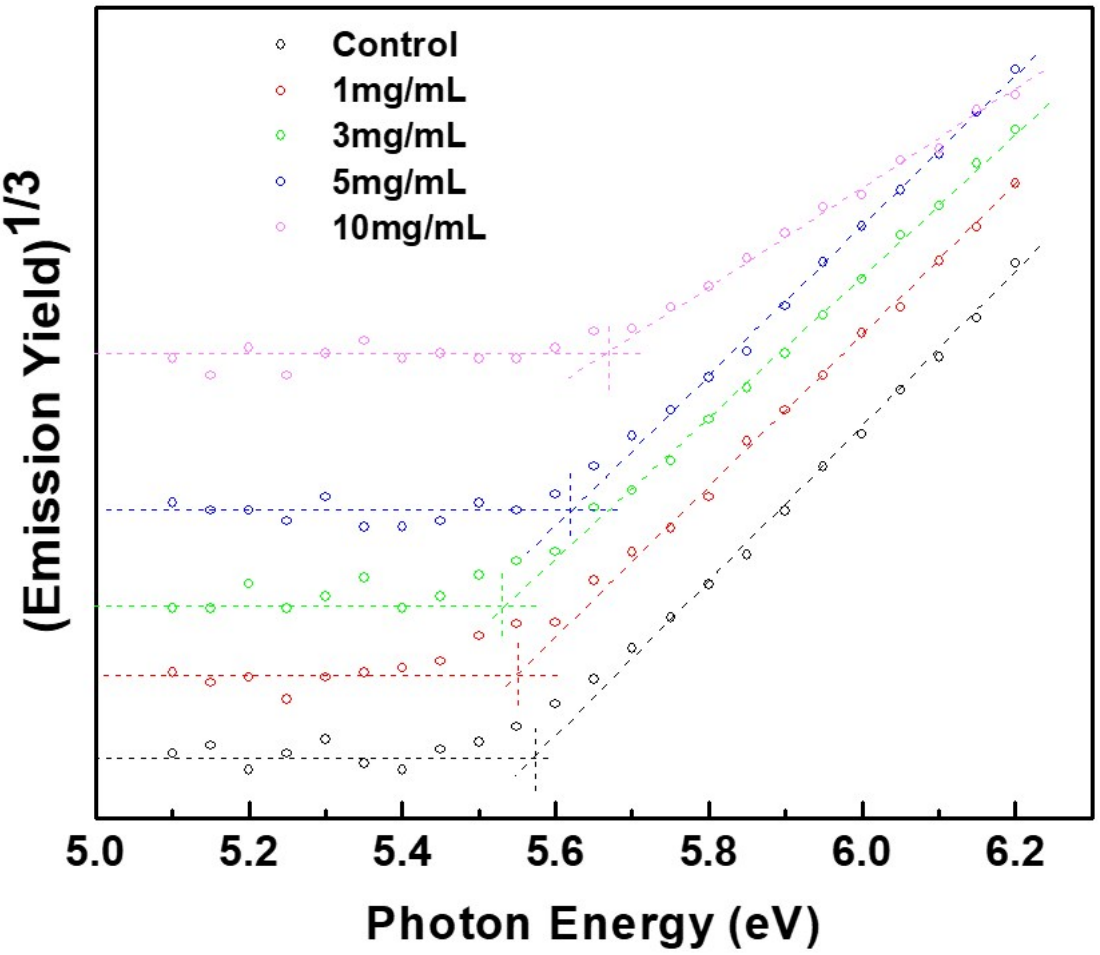

Fig. S6. The spectra of photo electron spectroscopy in air (PESA) of perovskite films on glass substrate.

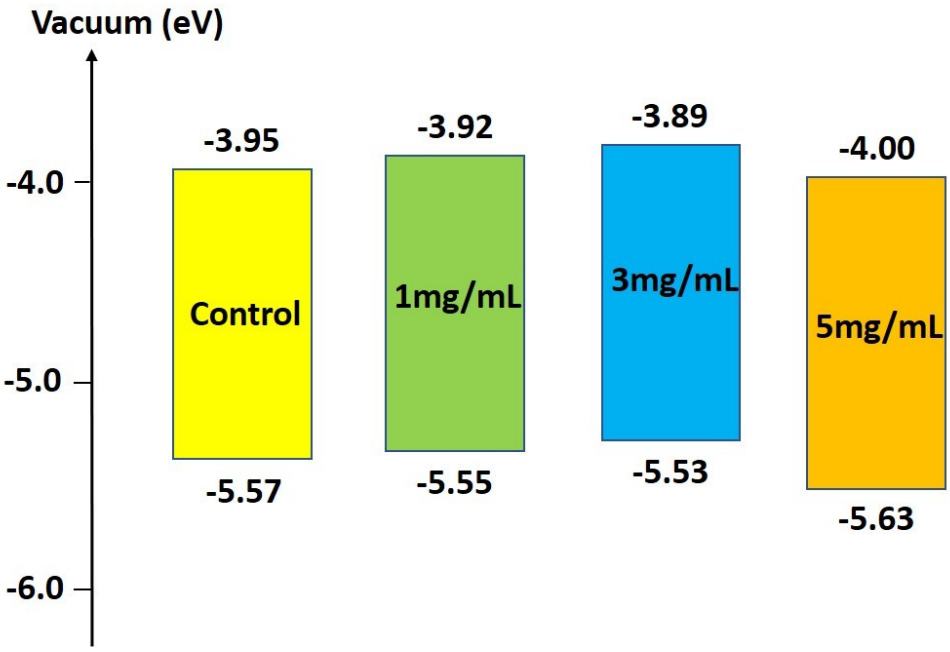

Fig. S7. Estimated bandgap edge position of perovskite. The band position of the 10 mg/ml FACl loading film is not available here due to the rapid degradation occurred throughout the experiments.

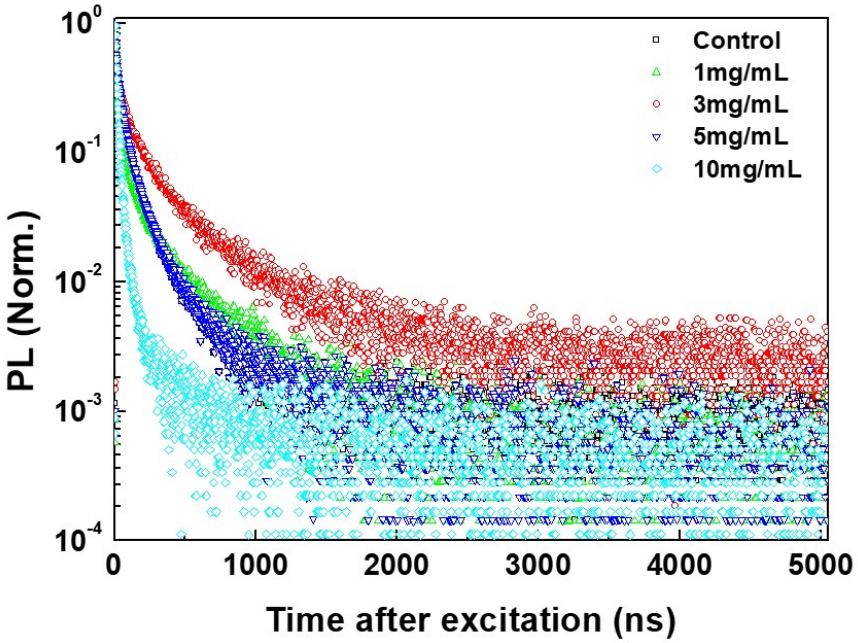

Fig. S8. Time-resolved photoluminescence decay after excitation at 507 nm (pulsed with 200 kHz and a fluence of 30 nJ cm^{-2} per pulse).

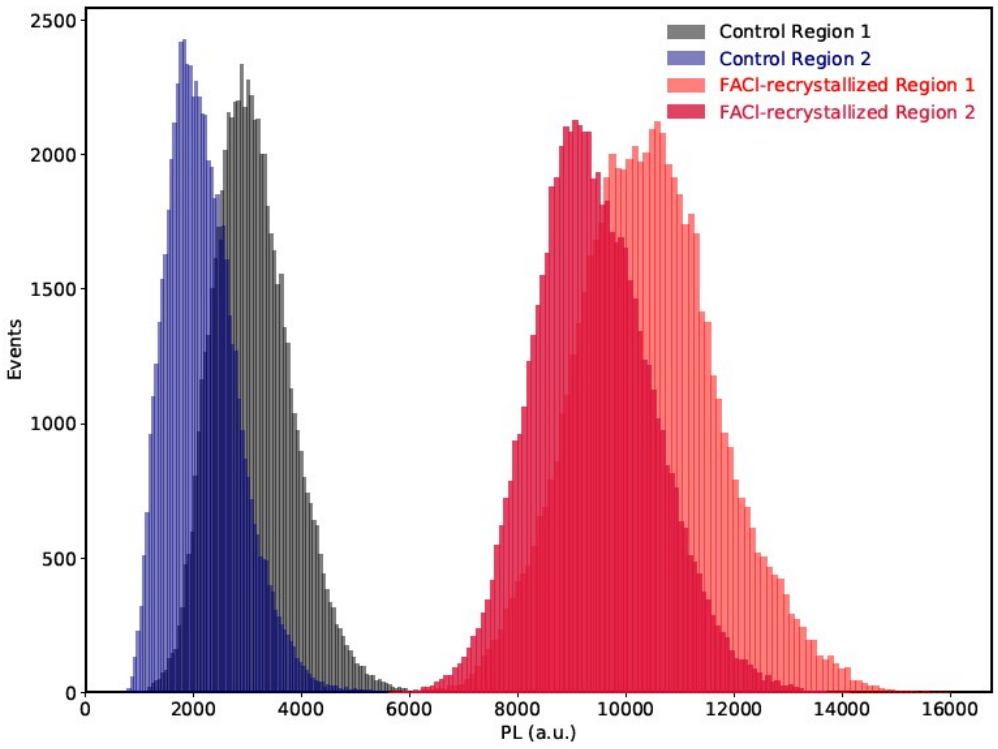

Fig. S9. Image histograms (65,536 total pixels) of fluorescence maps taken in two different regions in a control film and two different regions in a FACl-recrystallized film showing the fluorescence emission distribution. Region 1 correspond to the histograms reported in the main article, and Region 2 are new areas that also demonstrate both a higher average photoluminescence intensity and more homogeneous fluorescence emission distribution after FACl recrystallization.

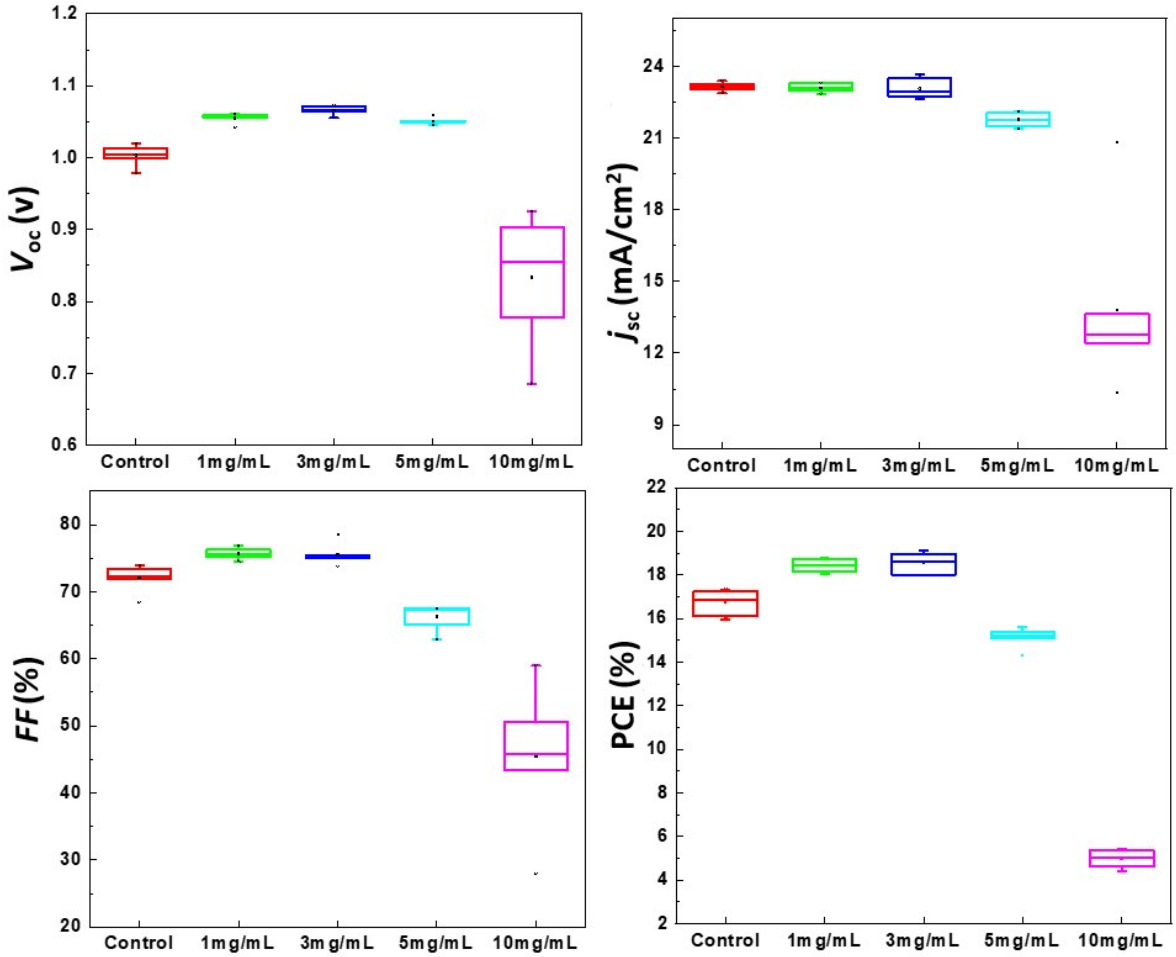

Fig. S10. Statistical distribution of photovoltaic parameters extracted from the *j-V* curves of devices with different concentration of FACl loading.

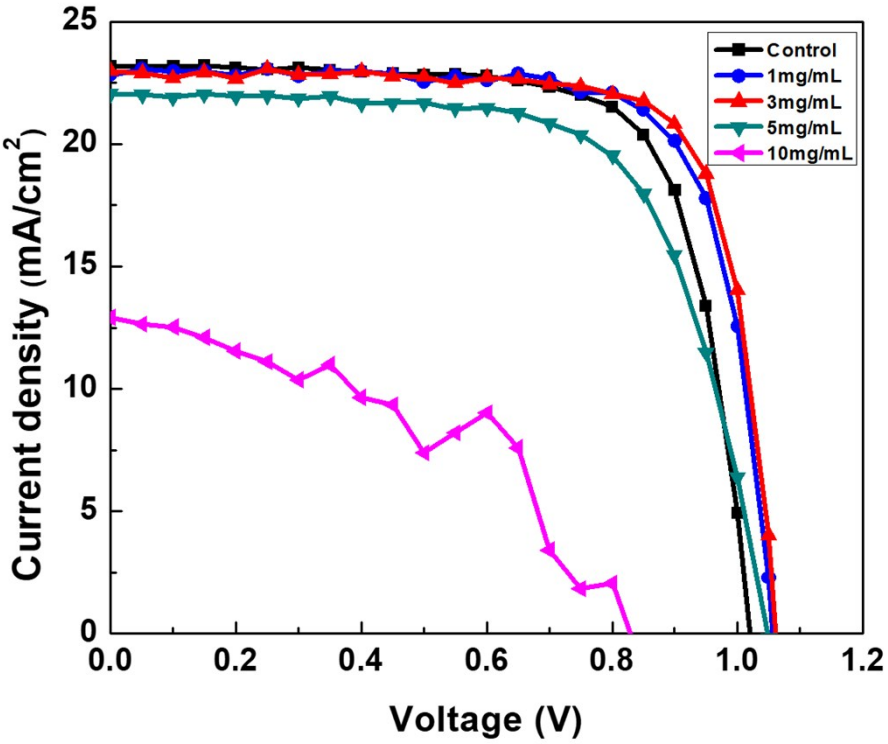

Fig. S11. *j-V* curves of control and a series of FACl-treated devices (1 sun illumination, aperture area = 0.08 cm^2).

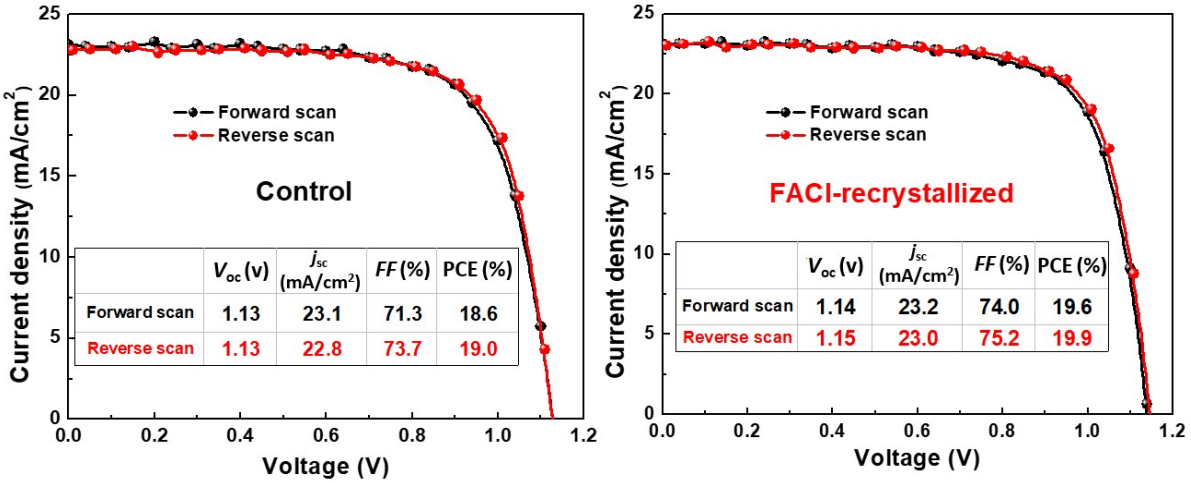

	V_{oc} (v)	j_{sc} (mA/cm^2)	*FF* (%)	PCE (%)
Forward scan	1.13	23.1	71.3	18.6
Reverse scan	1.13	22.8	73.7	19.0

	V_{oc} (v)	j_{sc} (mA/cm^2)	*FF* (%)	PCE (%)
Forward scan	1.14	23.2	74.0	19.6
Reverse scan	1.15	23.0	75.2	19.9

Fig. S12. *j-V* hysteresis behavior in typical Control and FACl-recrystallized devices.

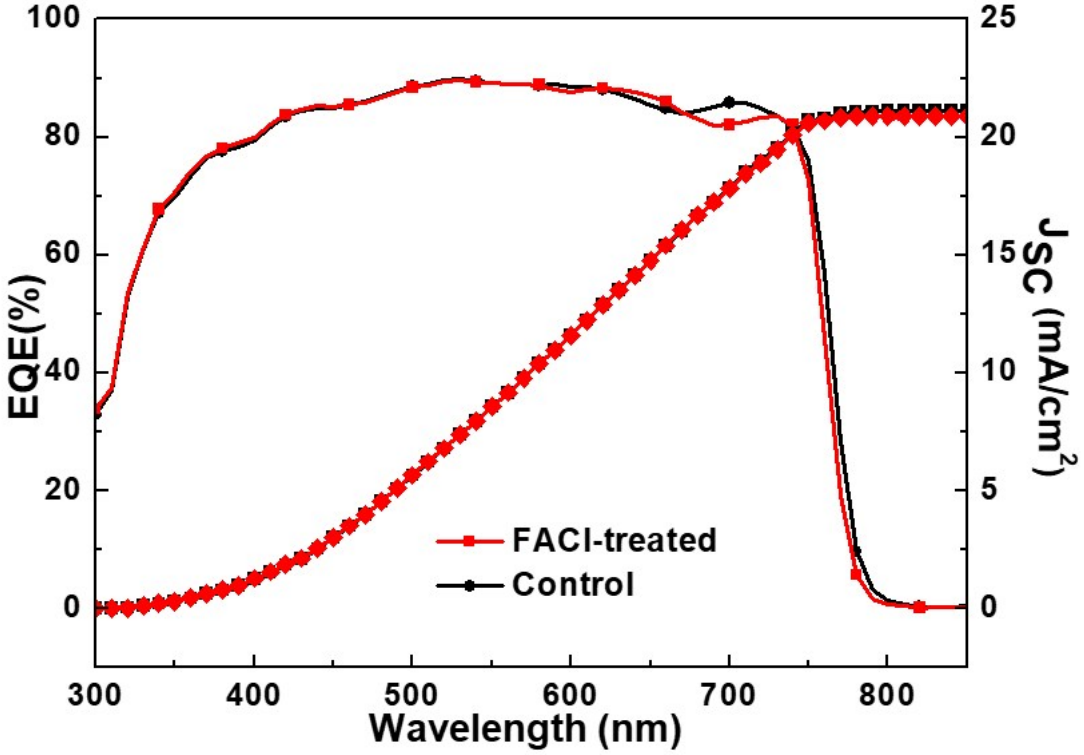

Fig. S13. EQE spectrum of the control cell and with FACl-recrystallized cells.

Note on integrated EQE presented in Fig. S13

The slight difference between the EQE-integrated j_{SC} and the *j-V* measurement-extracted j_{SC} is attributed to experimental uncertainties introduced by using an EQE system with an under-illuminating monochromatic beam. The under-illuminating beam may not correctly estimate the reference cell EQE [5,6] which results in a wavelength independent scaling error in the measured EQE value. Any error from this source will apply to all measured devices equally as all are referenced using the same system.

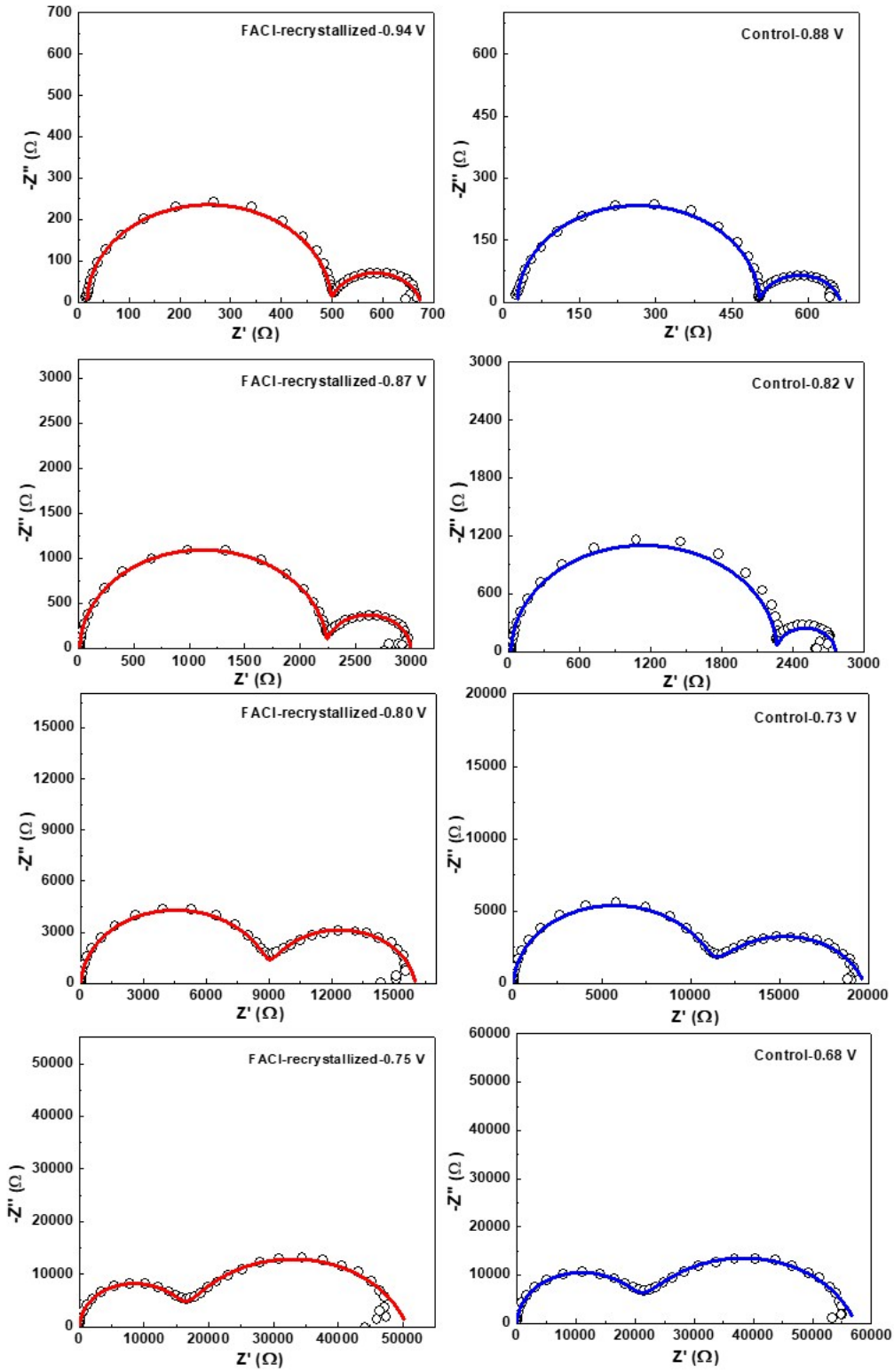

Fig. S14. Nyquist plots of the perovskite devices measured under illumination with different light intensity.

	Control	1mg/mL	3mg/mL	5mg/mL
Band-gap (eV)	1.617	1.626	1.638	1.621

Table S2. Related to calculation results of Band-gap energies from Fig. S5.

	Control	1mg/mL	3mg/mL	5mg/mL	10mg/mL
Valance Band (eV)	5.57	5.55	5.53	5.63	5.67

Table S3. Related to valance band extracted from Fig. S6.

Sample	V_{OC} (V)	j_{SC} (mA/cm^2)	*FF* (%)	PCE (%)
Control	1.00±0.01	23.14±0.17	72.03±1.95	16.73±0.57
1 mg/mL	1.06±0.01	23.09±0.19	75.69±0.83	18.44±0.31
3 mg/mL	1.07±0.01	23.06±0.42	75.55±1.62	18.57±0.50
5 mg/mL	1.05±0.01	21.76±0.29	66.26±1.94	15.15±0.44
10 mg/mL	0.83±0.09	13.81±3.60	45.44±10.32	4.97±0.40

Table S4. Related to performance parameters extracted from Fig. S10.

Sample	V_{OC} (V)	j_{SC} (mA/cm^2)	*FF* (%)	PCE (%)
Control	1.02	23.16	73.31	17.33
1 mg/mL	1.06	22.98	76.89	18.75
3 mg/mL	1.07	22.75	78.55	19.15
5 mg/mL	1.05	22.06	67.51	15.61
10 mg/mL	0.83	12.90	50.62	5.41

Table S5. Related to performance parameters extracted from Fig. S11.

Sample	V_{OC} (V)	j_{SC} (mA cm^{-2})	*FF* (%)	PCE (%)
Control	1.13 ± 0.01	22.7 ± 0.21	73.8 ± 0.9	18.98 ± 0.3
FACl-recrystallized	1.14 ± 0.01	22.7 ± 0.24	76.1 ± 1.1	19.64 ± 0.3

Table S6. Related to the mean device performance parameters of a batch of solar cells devices extracted from *j-V* curves in Fig. 4b under simulated AM 1.5, 100 mW/cm^2 solar irradiation.

REFERENCES

1 E. H. Anaraki, A. Kermanpur, L. Steier, K. Domanski, T. Matsui, W. Tress, M. Saliba, A. Abate, M. Grä, A. Hagfeldt and J.-P. Correa-Baena, *Energy Environ. Sci.*, 2016, **3128**, 3128–3134.

2 S. D. Stranks, S. D. Stranks, G. E. Eperon, G. Grancini, C. Menelaou, M. J. P. Alcocer, T. Leijtens, L. M. Herz, A. Petrozza and H. J. Snaith, *Science*, 2014, **342**, 341–344.

3 J. C. de Mello, H. F. Wittmann and R. H. Friend, *Adv. Mater.*, 1997, **9**, 230–232.

4 J. Tauc, Ed., *Amorphous and Liquid Semiconductors*, Springer US, Boston, MA, 1974.

5 Henry J. Kostkowski, *Reliable Spectroradiometry*, La Plata, Md., 1997.

6 K. Emery, D. Dunlavy, H. Field and T. Moriarty, *July*, 1998, **6**, 5.